

# DYNAMICAL EFFECTS DUE TO FRINGE FIELD OF THE MAGNET IN CIRCULAR ACCELERATORS<sup>\*</sup>

Y. Cai<sup>†</sup>, Y. Nosochkov, SLAC, Menlo Park, CA 94025, USA

## Abstract

The leading Lie generators, including the chromatic effects, due to hard-edge fringe field of single multipole and solenoid are derived from the vector potentials within a Hamiltonian system. These nonlinear generators are applied to the interaction region of PEP-II to analyze the linear errors due to the feed-down from the off-centered quadrupoles and solenoid. The nonlinear effects of tune shifts at large amplitude, the synchro-betatron sidebands near half integer and their impacts on the dynamic aperture are studied in the paper.

## INTRODUCTION

PEP-II is an asymmetric B-factory that consists of two separate rings with different energies. The electron and positron beams are brought into head-on collisions at the BABAR detector as shown in Fig. 1. In order to separate the beams fast enough away from the interaction point (IP) to avoid the deteriorating effect on the luminosity due to adjacent parasitic collisions, the beams go through many strong magnets inside the solenoid with very large offsets from their center. These offsets can be as large as a few centimeters as indicated in Fig. 1. The excursion of the design orbit introduces large uncertainty into the optics near the IP. Most problematic, the optics changes, as recently seen in the beam-beam experiments [1], when the local orbit varies.

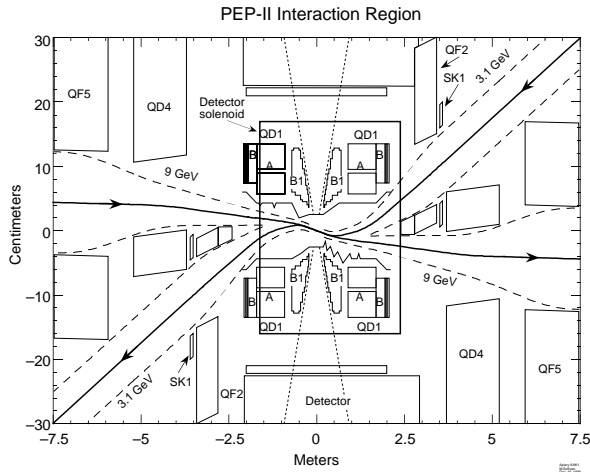


Figure 1: Top view of the PEP-II magnets and detector solenoid near the interaction point.

An accurate optical model requires a map of three-dimensional magnetic field in the region. That is rather difficult to compute because of the overlapping fields and complicated geometry. As a first step, we will use the hard-edge model for the fringe field to estimate the effects analytically in this paper.

## VECTOR POTENTIAL

The magnetic field of a single normal harmonics, including its fringe field, in the cylindrical coordinate is derived by Bassetti and Biscari [2]. To study the single-particle effects of the fringe field using Hamiltonian system, we need to know its corresponding vector potential.

### Single normal harmonics, $n > 0$

In the Coulomb gauge,  $\nabla \cdot \vec{A} = 0$ , the potential can be expressed as

$$\begin{aligned} A_r &= \frac{\cos n\theta}{2n!} \sum_{p=0}^{\infty} \frac{1}{n+p+1} G_{n,2p+1}(s) r^{2p+n+1}, \\ A_\theta &= \frac{\sin n\theta}{2n!} \sum_{p=0}^{\infty} \frac{1}{n+p+1} G_{n,2p+1}(s) r^{2p+n+1}, \\ A_s &= -\frac{\cos n\theta}{n!} \sum_{p=0}^{\infty} G_{n,2p}(s) r^{2p+n}, \end{aligned} \quad (1)$$

where

$$\begin{aligned} G_{n,2p}(s) &= (-1)^p \frac{n!}{4^p (n+p)! p!} \frac{d^{2p} G_{n,0}(s)}{ds^{2p}}, \\ G_{n,2p+1}(s) &= \frac{dG_{n,2p}(s)}{ds}. \end{aligned} \quad (2)$$

For a skew multipole, the expression can be obtained by an exchange between sine and cosine. The Coulomb gauge is chosen because its potential becomes the conventional multipole expansion.

### Solenoid, $n = 0$

For the solenoid, due to its axial symmetry, it is more convenient to choose the axial gauge:  $A_s = 0$ . The vector potential is given by

$$\begin{aligned} A_x &= -\frac{y}{2} \sum_{p=0}^{\infty} \frac{1}{p+1} G_{0,2p+1} r^{2p}, \\ A_y &= \frac{x}{2} \sum_{p=0}^{\infty} \frac{1}{p+1} G_{0,2p+1} r^{2p}. \end{aligned} \quad (3)$$

The potential satisfies Maxwell's equation  $\nabla \times \nabla \times \vec{A} = 0$ . Any truncation of the series could violate Maxwell's equation. The magnetic field is given by  $\vec{B} = \nabla \times \vec{A}$ .

<sup>\*</sup> Work partially supported by the Department of Energy under Contract No. DE-AC02-76F00515.

<sup>†</sup> yunhai@slac.stanford.edu

## HARD-EDGE FRINGE

In the Cartesian coordinate system, the Hamiltonian, using the distance  $s$  as the independent variable for a charged particle moving in a static magnetic field, is given by [3]

$$H(x, p_x, y, p_y, \delta, l; s) = -a_s - \sqrt{(1 + \delta)^2 - (p_x - a_x)^2 - (p_y - a_y)^2}, \quad (4)$$

where  $a_{x,y,s} = eA_{x,y,s}/cp_0$  are scaled components of the vector potential along axis  $x, y, s$ , respectively;  $p_x, p_y$  are the transverse canonical momenta scaled by a reference momentum  $p_0$ ,  $\delta = (p - p_0)/p_0$ , and  $l = vt$  is the path length. We expand the square root in Eq. (4) and keep only the first order of the vector potential,

$$H = -(1 + \delta) + \frac{1}{2(1 + \delta)}(p_x^2 + p_y^2) - [a_s + \frac{1}{1 + \delta}(p_x a_x + p_y a_y)]. \quad (5)$$

This Hamiltonian is used to compute the dynamical effects on the charged particles due to the fringe field.

### Solenoid

Taking a solenoid with field  $B_s$  as an example and follow the method used by Forest and Milutinovic [5], we choose a hard-edge model

$$G_{0,1} = B_s \theta(s), \quad (6)$$

where  $\theta(s)$  is the unit step function. Using this model and the vector potential in Eq. (3), we have,  $A_s = 0$  and

$$\begin{aligned} A_x &= -\frac{y}{2}\{B_s \theta(s) - \frac{B_s}{8}(x^2 + y^2)\theta''(s) + \dots\} \\ A_y &= \frac{x}{2}\{B_s \theta(s) - \frac{B_s}{8}(x^2 + y^2)\theta''(s) + \dots\}. \end{aligned} \quad (7)$$

Substituting these components into the Hamiltonian in Eq. (5), we obtain

$$H = D + V_0 \theta(s) + V_2 \theta''(s), \quad (8)$$

where

$$\begin{aligned} D &= -(1 + \delta) + \frac{1}{2(1 + \delta)}(p_x^2 + p_y^2), \\ V_0 &= \frac{K_s}{2(1 + \delta)}(yp_x - xp_y), \\ V_2 &= \frac{K_s}{16(1 + \delta)}(yp_x - xp_y)(x^2 + y^2), \end{aligned} \quad (9)$$

and  $K_s = eB_s/cp_0$ . After the standard manipulation of map and integration by parts [5], we obtain the map

$$\mathcal{M}_s = e^{:[V_2, D]:} = e^{:f_s:},$$

where

$$f_s = \frac{K_s}{8(1 + \delta)^2}[xy(p_x^2 - p_y^2) + p_x p_y (y^2 - x^2)] \quad (10)$$

Here,  $:f : g = [f, g]$  and  $[, ]$  denotes the Poisson bracket. Note that  $\mathcal{M}_s$  is invariant under the two-dimensional rotation around the axis of the solenoid.

### Dipole

Similarly, for a dipole magnet, we start with

$$G_{1,0} = B_0 \theta(s), \quad (11)$$

and set  $n = 1$  in Eq. (1) to obtain the components of the vector potential of a dipole magnet as follows

$$\begin{aligned} A_x &= \frac{1}{2}(x^2 - y^2)\{\frac{1}{2}B_0 \theta'(s) + \dots\}, \\ A_y &= xy\{\frac{1}{2}B_0 \theta'(s) + \dots\}, \\ A_s &= -x\{B_0 \theta(s) - \frac{B_0}{8}(x^2 + y^2)\theta''(s) + \dots\}, \end{aligned}$$

where  $B_0$  is the magnetic field of the dipole. The Hamiltonian is derived by substituting the vector potential into Eq. (5). We have

$$H = D + V_0 \theta(s) + V_1 \theta'(s) + V_2 \theta''(s), \quad (12)$$

where

$$\begin{aligned} D &= -(1 + \delta) + \frac{1}{2(1 + \delta)}(p_x^2 + p_y^2), \\ V_0 &= \frac{x}{\rho}, \\ V_1 &= -\frac{1}{1 + \delta}[\frac{p_x}{4\rho}(x^2 - y^2) + \frac{p_y}{2\rho}xy], \\ V_2 &= -\frac{x}{8\rho}(x^2 + y^2), \end{aligned} \quad (13)$$

and  $1/\rho = eB_0/cp_0$  and  $\rho$  is the bending radius of the dipole magnet. The final map is written as

$$\mathcal{M}_d = e^{:-V_1 + [V_2, D]:} = e^{:f_d:}, \quad (14)$$

where,

$$f_d = \frac{1}{8\rho(1 + \delta)}[-x^2 p_x + 2xy p_y - 3y^2 p_x]. \quad (15)$$

As a first-order kick and  $\delta = 0$ , it agrees with the expression found by Papaphilippou, Wei, and Talman [4].

### Quadrupole

Similar exercise can be carried out for a quadrupole magnet with  $n = 2$ . The final map is given by

$$\mathcal{M}_q = e^{:f_q:}, \quad (16)$$

where,

$$f_q = \frac{K_1}{12(1 + \delta)}[-(x^3 + 3xy^3)p_x + (y^3 + 3yx^2)p_y]. \quad (17)$$

where  $K_1 = eG/cp_0$  and  $G$  is the gradient.  $\mathcal{M}_q$  agrees with the expression first found by Forest and Milutinovic.

Here, the maps are derived for the raising edge of the magnet. For the falling edge, the maps are obtained by simply switching the sign of the Lie generator of the map.

If there is a design off-axis orbit:  $\Delta x$  and  $\Delta p_x$  in the horizontal plane, the non-linear effects of the fringe field of

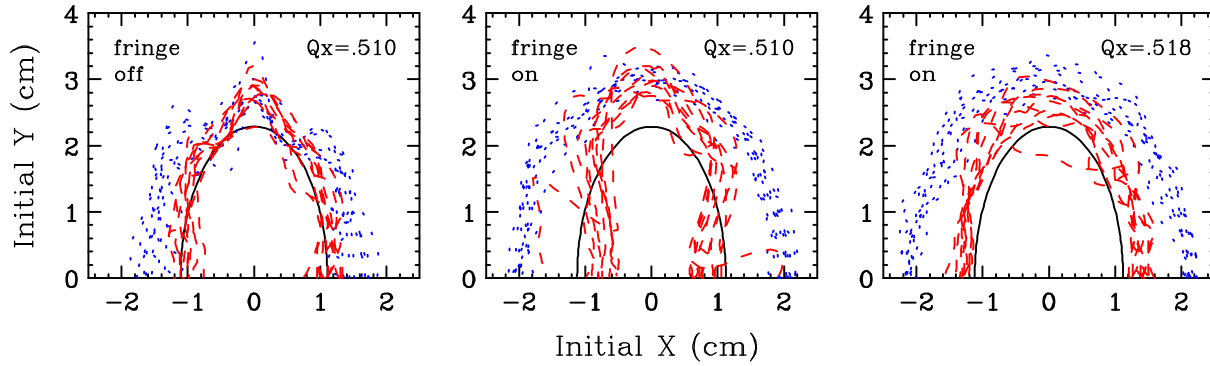


Figure 2: Evolution of HER dynamic aperture with quadrupole nonlinear fringe off and on at  $\nu_x = .510$  and  $.518$ .

Table 1: Tune shift from the quadrupole adjacent to the IP.

Name	s(m)	$\Delta x(mm)$	$\Delta p_x(mrad)$	$\Delta \nu_y$
QD1L-U	-2.06	-30.54	46.61	$8.1 \times 10^{-3}$
QD1L-D	-0.90	5.01	11.38	$2.3 \times 10^{-4}$
QD1R-U	0.90	-5.01	11.38	$2.3 \times 10^{-4}$
QD1L-D	2.06	30.00	46.38	$8.1 \times 10^{-3}$

a quadrupole magnet will feed down to linear optical errors. By substituting  $x$  with  $x + \Delta x$  and  $p_x$  with  $p_x + \Delta p_x$  into Eq. (17), and extracting the quadratic terms of  $x, p_x, y, p_y$ , we find that the tune shifts are given by

$$\begin{aligned} \Delta \nu_x &= \frac{K_1}{8\pi(1+\delta)} (\Delta x \Delta p_x \beta_x - \Delta x^2 \alpha_x), \\ \Delta \nu_y &= \frac{K_1}{8\pi(1+\delta)} (\Delta x \Delta p_x \beta_y + \Delta x^2 \alpha_y), \end{aligned} \quad (18)$$

where  $\beta$  and  $\alpha$  are the Courant-Snyder parameters at the position of the edge. For PEP-II, the estimated tune shifts in the vertical plane relative to the design orbit in the Low Energy Ring are tabulated in Table 1.

Note that the outside edges of the quadrupole contribute more because the excursions are larger. These rather large optical effects are not currently included in our optical model.

## NONLINEAR EFFECTS

The nonlinear fringe transformation at quadrupole edges has been recently implemented in the LEGO code [6]. Based on Eq. (17), the fringe octupole-like field would generate an amplitude dependent tune shift and excite chromogeometric octupole resonances. These effects were observed in PEP-II dynamic aperture calculations. To maximize luminosity, the PEP-II horizontal tune is moved close to a half-integer. However, the tune space in this region is limited by the effects of half-integer resonance and its synchrotron side bands. The effect of the quadrupole resonances on PEP-II dynamic aperture had been observed in earlier tracking studies [7]. In this case, the resonance condition is  $2\nu_x + k\nu_s = n$ , where  $\nu_s$  is the synchrotron tune.

After including the nonlinear fringe in quadrupoles, the tracking showed a reduction of dynamic aperture for off-

momentum particles. An example of dynamic aperture for PEP-II High Energy Ring (HER) is shown in Fig. 2. In this case, the  $90^\circ$  HER upgrade lattice [8] is used where the IP beta functions and tunes are  $\beta_x^*/\beta_y^* = 50/1$  cm and  $\nu_x/\nu_y/\nu_s = 28.51/27.63/0.0405$ . The tracking included synchrotron oscillations, machine errors and various optics corrections. In Fig. 2, the blue dotted lines show on-momentum dynamic aperture for 10 random error settings, the dash red lines correspond to relative momentum error of  $\delta = 8\sigma_\delta$ , and the solid ellipse shows the  $10\sigma$  beam size for reference. One can see that the fringe effect increases the on-momentum aperture but reduces the horizontal off-momentum aperture at  $.510$  tune. The on-momentum improvement is due to the fringe compensation of the amplitude dependent tune shift from sextupoles. The off-momentum effect was attributed to the 1st octupole side band of the half-integer resonance excited by the fringe. In this case, the octupole resonance condition  $4\nu_x + l\nu_s = 114$  yields the resonance tune at  $\nu_x = 28.5101$ . Moving the tune away from this resonance to  $28.518$  restored the aperture above the  $10\sigma$  size.

## CONCLUSION

We have found a new Lie generator for the hard-edge fringe due to a solenoid magnet. It is a fourth-order generator and gives an octupole-like kick to charge particles. It can also provide additional x-y couplings through an off-centered orbit.

## REFERENCES

- [1] W. Kozanecki *et al.*, "Experimental Study of Crossing-Angle and Parasitic Crossing Effects at the PEP-II  $e^+e^-$  Collider," PAC'05, these proceedings.
- [2] M. Bassetti and C. Biscari, PA **52**, 221 (1996).
- [3] R. Ruth, AIP Conference Proceedings No. 153, Vol.1 p166, M. Month and M. Dienes editors (1985).
- [4] Y. Papaphilippou, J. Wei, and R. Talman, Phys. Rev. E **67**, 046502 (2003).
- [5] E. Forest and J. Milutinovic, Methods Phys. Res. **A269**, 474 (1988).
- [6] Y. Cai, *et al.*, SLAC-PUB-7642 (1997).
- [7] Y. Cai, Y. Nosochkov, SLAC-PUB-9812 (2003).
- [8] Y. Cai, *et al.*, SLAC-PUB-9810 (2003).